Supplementary information of "Inorganic SnIP-Type Double Helices: Promising Candidates for High-Efficiency Photovoltaic Cells"

Haozhe Li[1,2], Xin-Gao Gong[1,2], and Ji-Hui Yang[1,2†]

[1]Key Laboratory for Computational Physical Sciences (MOE), Department of Physics, Fudan University, Shanghai 200433, China

[2]Shanghai Qizhi Institution, Shanghai 200232, China

Contents

Table S1. Lattice constants (Å), volume of unit cell ($Å^3$), average bond lengths of X-Y (Å) and Pn-Pn (Å) for double helical bulk XYPn compounds.

Bulk	SiClP	SiBrP	SiIP	GeClP	GeBrP	GeIP
a	7.40	7.40	7.41	7.66	7.66	7.67
b	8.59	8.98	9.63	8.77	9.10	9.76
c	16.94	17.31	18.07	16.77	17.30	18.22
V	965.18	1058.85	1212.07	1013.32	1112.92	1278.95
X-Y	2.81	2.87	3.02	2.81	2.92	3.08
Pn-Pn	2.22	2.22	2.23	2.21	2.21	2.22
Bulk	SnClP	SnBrP	SnIP	SiClAs	SiBrAs	SiIAs
a	8.12	8.10	8.05	8.00	7.92	7.91
b	9.08	9.33	9.96	8.76	9.11	9.68
c	17.35	17.87	18.72	17.21	17.68	18.33
V	1156.75	1245.15	1404.46	1043.71	1143.80	1300.01
X-Y	2.97	3.01	3.19	2.85	2.93	3.06
Pn-Pn	2.20	2.21	2.21	2.47	2.48	2.48
Bulk	GeClAs	GeBrAs	GeIAs	SnClAs	SnBrAs	SnIAs
a	8.25	8.18	8.18	8.74	8.65	8.63
b	8.96	9.21	9.77	9.13	9.45	9.90
c	17.11	17.54	18.26	17.49	18.14	18.78
V	1084.26	1187.18	1352.82	1228.54	1333.03	1488.09
X-Y	2.84	2.98	3.15	2.92	3.11	3.25
Pn-Pn	2.46	2.46	2.47	2.46	2.46	2.47

Table S2. Indirect bandgaps/direct bandgaps (eV) of 18 XYPn compounds calculated

in different functionals (PBE, HSE06).

Bulk	SiClP	SiBrP	SiIP	SiClAs	SiBrAs	SiIAs
PBE	1.4013/	1.4764/	1.2335/	0.7758/	0.9881/	0.9715/
	1.4054	1.4992	1.2962	0.7770	0.9903	1.0023
HSE06	2.1705/	2.2279/	1.9342/	1.4077/	1.6520/	1.5930/
	2.1739	2.2516	1.9580	1.4123	1.6559	1.6256
Bulk	GeClP	GeBrP	GeIP	GeClAs	GeBrAs	GeIAs
PBE	1.6644/	1.7344/	1.5629/	1.0170/	1.1529/	1.2065/
	1.6804	1.7638	1.5978	1.0588	1.1669	1.2503
HSE06	2.4282/	2.4721/	2.2232/	1.6790/	1.8052/	1.8179/
	2.4446	2.5100	2.2574	1.6908	1.8210	1.8661
Bulk	SnClP	SnBrP	SnIP	SnClAs	SnBrAs	SnIAs
PBE	1.3007/	1.3983/	1.2722/	0.7928/	0.9161/	1.0077/
	1.3156	1.3996	1.2860	0.8456	0.9353	1.0097
HSE06	1.9633/	2.0548/	1.8617/	1.3509/	1.4983/	1.5623/
	1.9786	2.0581	1.8819	1.4108	1.5169	1.5647

Table S3. Calculated formation enthalpies (eV/formula) for $Sn_aI_bPn_c$(Pn = As, P) based on the HSE06 functional. The formation enthalpy of a binary compound is defined as $\Delta H_{X_aY_b} = E_{X_aY_b} - a \times E_X - b \times E_Y$, where $E_{X_aY_b}$ is the calculated energy of X_aY_b, $E_{X(Y)}$ is the energy of element X(Y) in its elemental solid or gas phase.

Compound	SnI_2	SnI_4	AsI_3	Sn_4As_3	SnIAs	/
$\Delta H_{Sn_aI_bAs_c}$	-0.68	-0.64	-0.39	-0.05	-0.36	/
Compound	SnI_2	SnI_4	PI_2	PI_3	Sn_4P_3	SnIP
$\Delta H_{Sn_aI_bP_c}$	-0.68	-0.64	-0.25	-0.27	0.03	-0.37

*We note that the calculated formation enthalpy of Sn_4P_3 is 0.032 eV/atom, which indicated that Sn_4P_3 might be thermodynamically unstable. Our calculation result

is consistent with the data provided by the Materials Project database[1], which also reveals that the calculated formation enthalpy of Sn_4P_3 in r2SCAN metaGGA functional is positive, i.e., 0.008 eV/atom. Considering the relatively small formation energy and the truth that Sn_4P_3 has been experimentally synthesized, we think it will not influence the overall conclusion.

**The space groups of materials calculated are Sn($Fd\bar{3}m$, No.227), I($Immm$, No.71), P($P\bar{1}$, No.2), As($R\bar{3}m$, No.166), SnI_2($C12/m1$, No.12), SnI_4($P\bar{4}3m$, No.215), PI_2($P\bar{1}$, No.2), PI_3($P6_3$, No.173), AsI_3($R\bar{3}$, No.148), Sn_4As_3($R\bar{3}m$, No.166), and Sn_4P_3($R\bar{3}m$, No.166). We have also used black phosphorus ($Cmce$, No.64) to calculate formation enthalpy and got the same conclusion expect a -0.02 eV formation enthalpy of Sn_4P_3 and a slightly smaller stable region for SnIP.

Fig. S1 The PBE bandgap of SnIAs with (b) and without (a) spin-orbit coupling (SOC) effect. The bandgap difference induced by SOC effect is $\Delta_{bandgap}$= 0.0318 eV. The overall features of band structures are same.

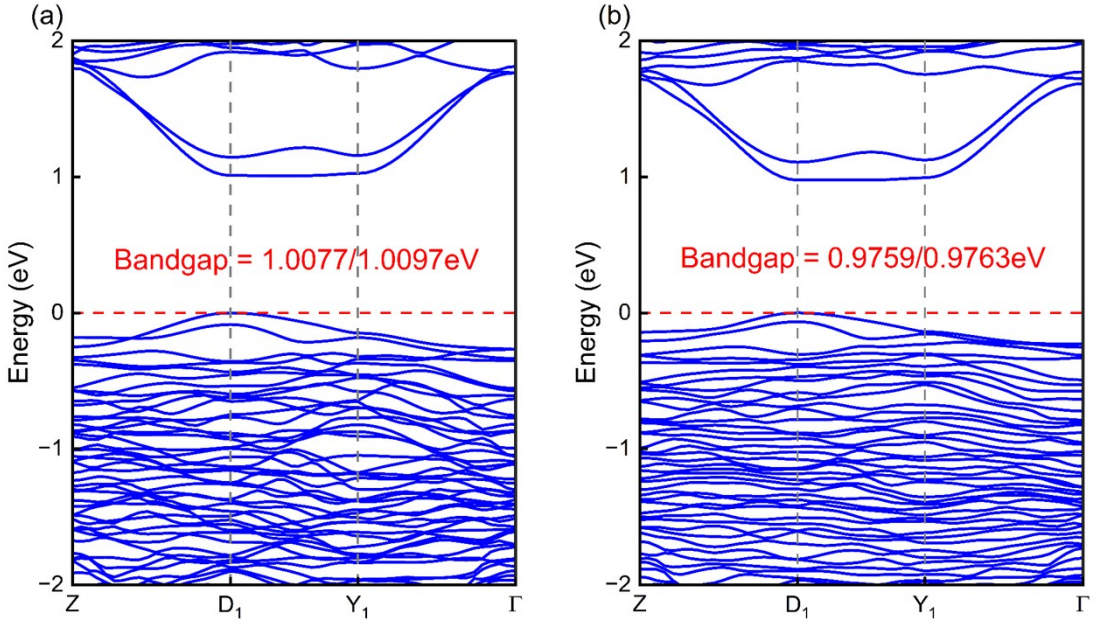

Fig. S2 The optimized crystal structures of 12 XYPn compounds with suitable bandgaps in the range of 0.8-2.0 eV. Among these compounds, only SiIP, SnClP, SnIP, SiIAs, GeIAs and SnIAs have double helical structures like SnIP.

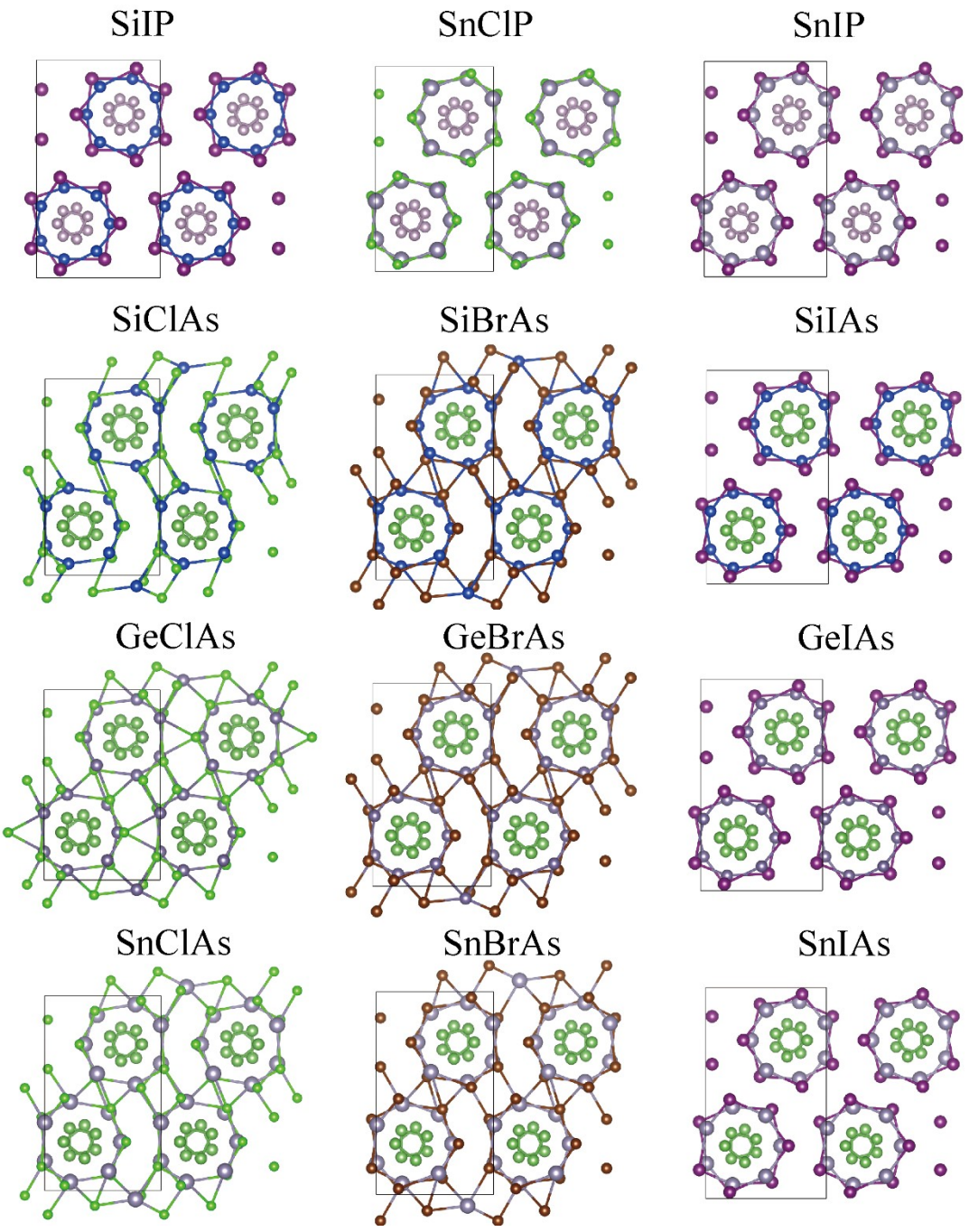

Fig. S3 The phonon dispersion spectra of six double helical structures (SiIP, SnClP, SnIP, SiIAs, GeIAs, SnIAs). We observed imaginary frequencies in SiIP, SnClP, SiIAs and GeIAs, which indicated possibly dynamic instability.

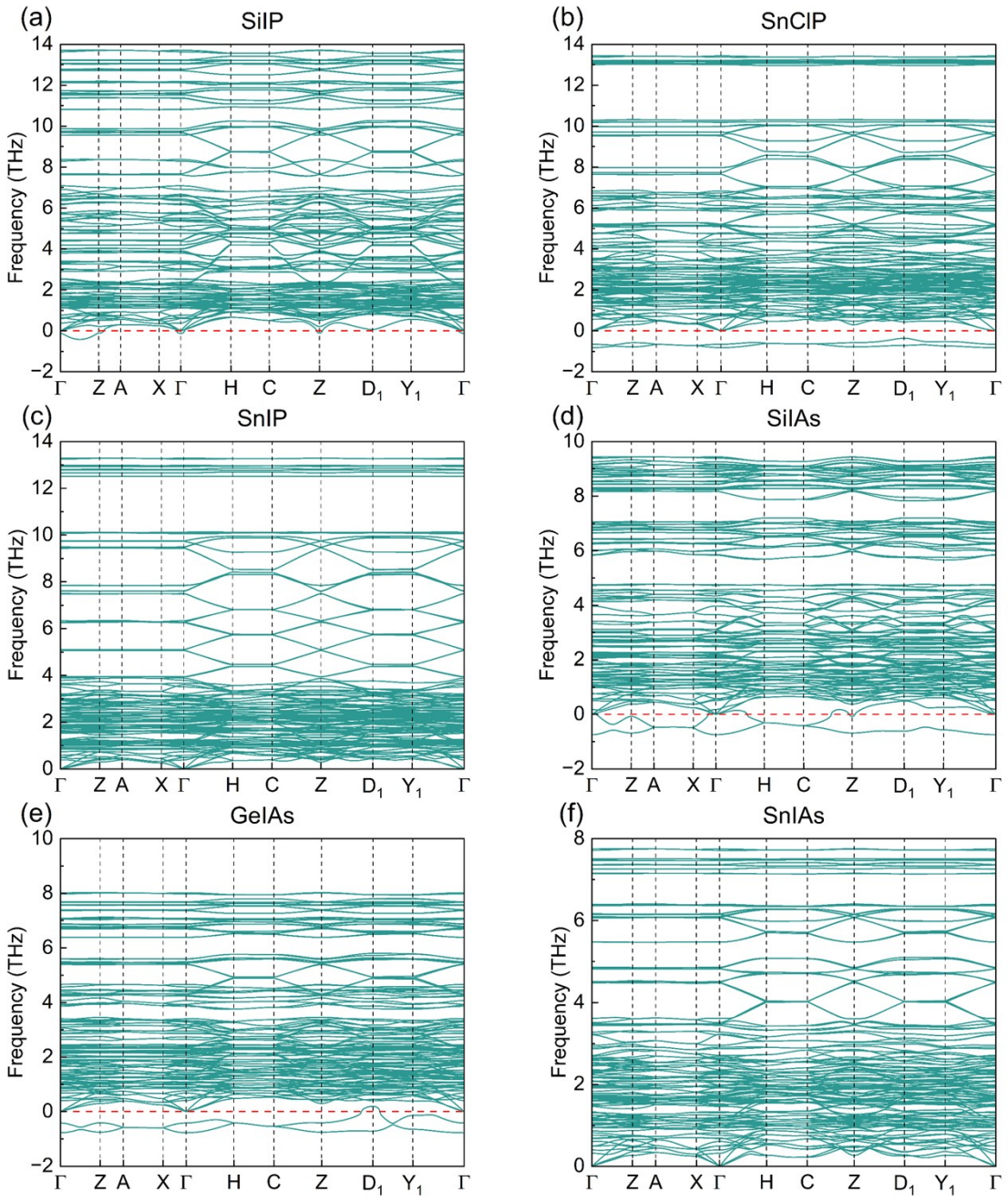

Note.1 The calculation of solar cell efficiency

The Spectroscopic Limited Maximum Efficiency (SLME) is proposed by Yu and Zunger[2], which includes the absorption coefficient and the absorber layer thickness in the efficiency assessment. Theoretically, the maximum solar cell efficiency is defined as

$$\eta = \frac{P_{max}}{P_{in}},$$

where P_{max} is the maximum power density generated by the solar cells and P_{in} is the

total incident power density from the solar irradiation. The P_{max} is derived by using the J-V curve of the solar cell:

$$P = JV = (J_{sc} - J_0(e^{\frac{eV}{kT}} - 1))V,$$

where k is the Boltzmann's constant. The short circuit current density J_{sc} is given by

$$J_{sc} = e\int_0^{\infty} a(E)I_{sun}(E)dE,$$

where e is the elementary charge, $a(E)$ is the photo absorptivity. $I_{sun}(E)$ is the AM 1.5G solar spectrum. The reverse saturation current J_0 is given by

$$J_0 = \frac{J_0^r}{f_r} = \frac{e\pi}{f_r}\int_0^{\infty} a(E)I_{bb}(E,T)dE,$$

where $I_{bb}(E,T)$ is the black-body spectrum at *T*. J_0^r is the radiative recombination current density. The fraction of radiative recombination f_r is defined as

$$f_r = e^{-\frac{E_g^{da} - E_g}{kT}},$$

where E_g and E_g^{da} are the fundamental bandgap and direct allowed band gaps. The photo absorptivity $a(E)$ for an absorber layer of thickness *L* with the absorption coefficient $\alpha(E)$ is defined as
$a(E) = 1 - e^{-2\alpha(E)L}$.

The open-circuit voltage V_{oc} is defined as

$$V_{oc} = \frac{KT}{e}\ln\left(1 + \frac{J_{sc}}{J_0}\right),$$

and the fill factor FF is defined as

$$FF = \frac{P_{max}}{J_{sc}V_{oc}}.$$

Fig. S4 Thickness dependence of the short circuit current densities $J_{sc}s$ (a), open circuit

voltages $^{V_{oc}s}$ (b) and fill factors FFs (c) of ^{Sb_2Se_3}, ^{MAPbI_3}, SnIAs, and SnIP.

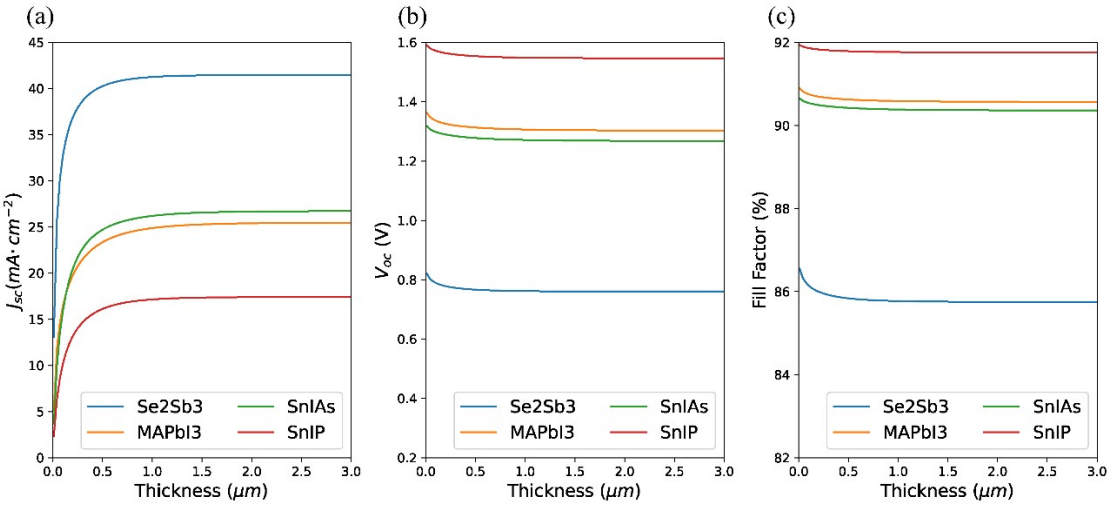

Fig. S5 Orbital character of the states close to the Fermi level of SnIAs. The VBM is mainly contributed by Sn-s (20%)/p (33%), I-p (33%), and As-p (14%) orbitals, while the CBM is mainly contributed by Sn-p (54%) and As-s (20%)/p (14%) orbitals. The data were calculated by the python package VASPKIT[3].

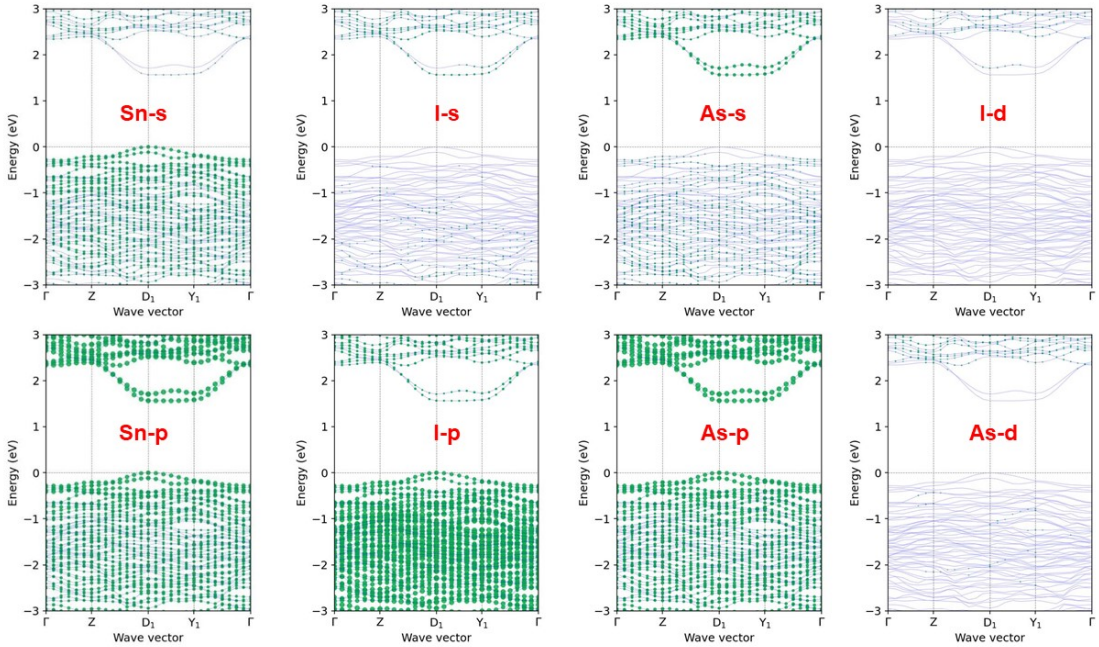

Fig. S6 Calculated thermodynamic phase diagram of the stable chemical potential regions for SnIP. The left panel is the enlarged view of the area in the right red box. The formulas on the right panel are the conditions for thermodynamic stability of SnIP.

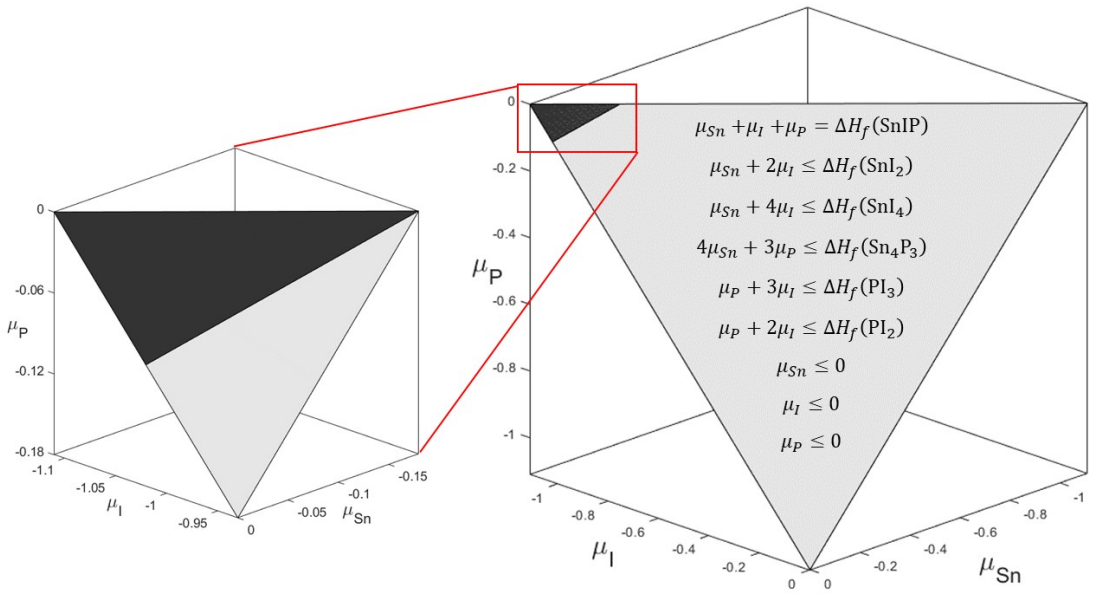

Fig. S7 (a) Calculated absorption coefficients as functions of light wavelengths for SnBrP, SnIAs, and SnIP. The AM1.5G solar irradiance spectrum is also shown for comparisons. (c) Simulated spectroscopic limited maximum efficiency (SLME) as functions of film thicknesses for SnBrP, SnIAs, and SnIP. The SLME of SnBrP at the scale of 1 μm is 21.12%.

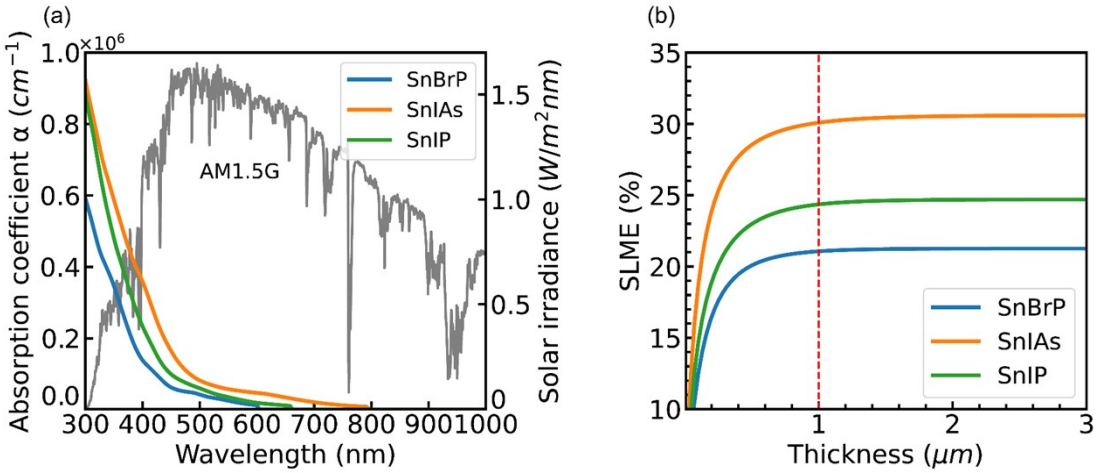

References

1 A. Jain, S. P. Ong, G. Hautier, W. Chen, W. D. Richards, S. Dacek, S. Cholia, D. Gunter, D. Skinner, G. Ceder and K. A. Persson, *APL Mater.*, 2013, **1**, 011002.

2 L. Yu and A. Zunger, *Phys. Rev. Lett.*, 2012, **108**, 068701.

3 V. Wang, N. Xu, J.-C. Liu, G. Tang and W.-T. Geng, *Comput. Phys. Commun.*, 2021, **267**, 108033.